



(RESEARCH ARTICLE)



Trend and Statistical Analysis of Photosynthetically Active Radiation (PAR) Across the Three Major Climatic Zones in Nigeria for 41 Years (1984–2024)

I. O. Ewona ^{1,2,*}, M. A. Okono ^{1,2}, E.O. Obi ^{1,2}, J. E. Osang ^{1,2} and J. A.Ushie ²

¹ Department of Physics, University of Calabar, Calabar, 540242, Nigeria.

² Department of Physics, University of Cross River State, Calabar, 540242, Nigeria.

International Journal of Science and Research Archive, 2025, 17(01), 444-454

Publication history: Received on 28 August 2025; revised on 07 October 2025; accepted on 10 October 2025

Article DOI: <https://doi.org/10.30574/ijrsra.2025.17.1.2768>

Abstract

Photosynthetically Active Radiation (PAR, 400–700 nm) is a key driver of photosynthesis, biomass formation, and crop yield, especially in the tropics where rainfed agriculture prevails. The present research examines the long-term variability and trends of PAR over Nigeria's three predominant climatic zones Humid Tropical Rainforest, Tropical Savanna, and Semi-Arid Sahel over a period of 41 years (1984–2024). NASA satellite-derived PAR data were examined using non-parametric statistical techniques such as Mann-Kendall trend detection test, Sen's slope estimator for rate estimation, and distribution-based analyses like kernel density estimation (KDE) and boxplots. Results show a statistically significant downward trend in PAR in all zones with Sen's slope ranging from -0.16 to -0.44 W/m^2 per year. The Humid Zone recorded the lowest PAR values due to constant cloud cover and excess rainfall, while the Tropical Savanna recorded mid-values, which were suitable for diverse cropping systems. The Semi-Arid Zone recorded the highest PAR levels but also with a significant decline, together with short wet seasons and high evapotranspiration. These declines in PAR have immediate consequences on agricultural productivity, ecosystem resistance, and food security, especially for staple crops like maize, sorghum, and millet that are radiation-sensitive. This study provides the first multi-decadal Nigeria-specific analysis of PAR trends for various climatic zones, and it offers important information to inform agricultural planning, climate adaptation, and policy development. Increased ground-level monitoring, adoption of climate-smart agriculture, and regional collaboration are recommended in an effort to mitigate the adverse impacts of reducing solar radiation on agriculture and livelihoods.

Keywords: Photosynthetically Active Radiation; PAR trends; Mann-Kendall; Sen's slope

1. Introduction

Solar radiation is the foundation of terrestrial productivity, climate, and ecosystem function, of which the Photosynthetically Active Radiation (PAR, 400–700 nm) fraction is the component essential for photosynthesis and crop yield [1][2]. In Nigeria, where rainfed agriculture supports over 60% of the population, PAR variability has significant implications for food security and socio-economic stability [3][4]. The country's latitudinal range from humid coastal rainforests to the semi-arid Sahel elicits intense contrasts in cloud cover, aerosols, and solar regimes, all of which impact PAR distribution [5][6].

The role of PAR in crop productivity was initially quantified by Monteith (1972)[7], who demonstrated a linear coincidence between absorbed PAR and yield, a finding subsequently verified in global productivity studies[8][9]. For C4 crops such as maize, sorghum, and millet, which are common in northern Nigeria, adequate PAR at flowering and grain filling is crucial. However, atmospheric modifiers such as biomass burning, Harmattan dust, and ozone fluctuations cause marked interannual variability in West Africa [10-14]. Udo & Aro (1999) [15] examined the relationship between global solar radiation (R_s) and photosynthetically active radiation (PAR) in Ilorin, Nigeria, and

* Corresponding author: M. A. Okono

found an annual mean PAR/Rs ratio of 2.08 E MJ^{-1} with marked seasonal variations. The ratio was lower during the dry Harmattan season (1.92 E MJ^{-1} in January) and higher in the rainy season (2.15 E MJ^{-1} in May), generally stabilizing around 2.1 E MJ^{-1} except in Harmattan months.

In spite of its significance, multi-decadal PAR analyses are still scant in Nigeria because of the paucity of radiometric networks. New developments in satellite datasets (e.g., MODIS, CERES) now enable vigorous trend determination. This research fills the gap by examining 41 years (1984–2024) of PAR variation in Nigeria's key climatic zones through Mann-Kendall, Sen's slope, KDE, and boxplots for trend evaluation and agricultural implications. The objectives are threefold: (i) to quantify long-term PAR trends across Nigeria's three principal climatic zones; (ii) to establish seasonal and interannual variability founded on stringent statistical protocols; and (iii) to examine implications for agriculture, environmental sustainability, and policy.

2. Data and Methods

2.1. Study Area

Nigeria lies between longitude 20E and 150 E and latitude 40 N and 140N, having two major seasons, wet and dry. The country is situated just above the geographical equator and this results to high sunshine intensity. This study is focused on the analysis of photosynthetically active radiation across the three major climatic zones in Nigeria. Figure1 shows all the selected states in Nigeria for across the climatic zones of the study which include the Humid Tropical Rain Forest zone, Tropical Savanna zone and Semi-Arid (Desert) zone. Table1 gives more information about each location.

Table 1 Study locations

Location	Elevation (m)	Latitude	Longitude
Humid Rain Forest			
Calabar	39.48	4.96	8.33
Warri	9.6	5.56	5.72
Lagos	25.49	6.55	3.34
Tropical Savanna			
Janligo	251.79	8.95	11.3
Lafia	180.63	8.51	8.51
Ilorin	344.93	8.52	4.53
Semi-Arid (Desert)			
Katsina	474.54	13.01	7.58
Sokoto	276.16	13.05	5.23
Maiduguri	318.25	11.89	13.13

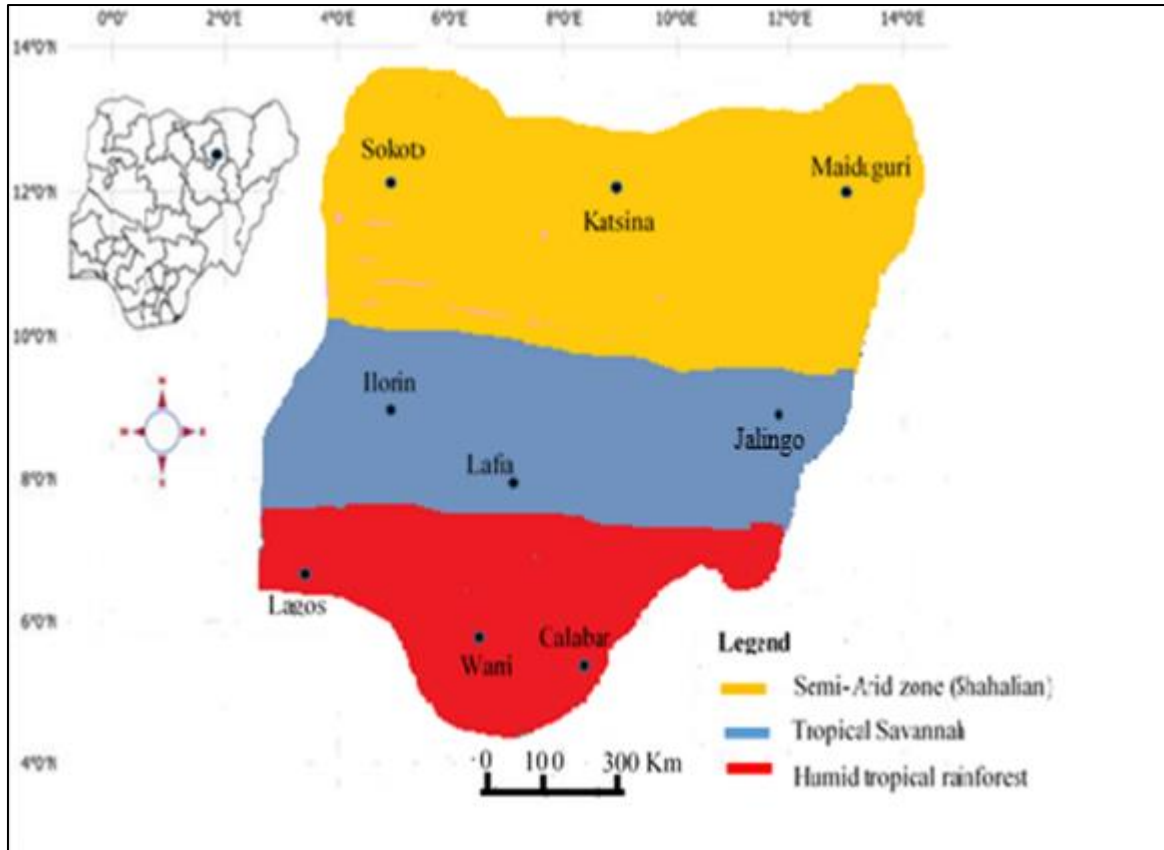


Figure 1 Map of Nigeria showing the three major climatic zones

2.2. Data Sources

PAR data were obtained from NASA database spanning 1984–2024. Data were aggregated into monthly and annual averages for each representative station.

2.3. Methods

The analysis tool for this study is the Microsoft Excel software, which was used for the data conversion, storage and wrangling. Data visualization was carried out by the Python programming language. All graphical representations and some statistical analysis were implemented. Packages in python programming like sklearn, seaborn, matplotlib, pandas, and numpy etc., were utilized for representations including box plots, linear regression,

2.3.1. Test for Trend (The Mann-Kendall Trend Test)

We use the M-K test when analysing time-series data. The test is non-parametric and does not require the data to conform to a particular distribution [16][17]. We apply this test when a given range of data agrees with the relation.

$$x_i = f(t_i) + \varepsilon_i \quad \dots\dots\dots (6)$$

$f(t_i)$ here is a function of continuously increasing or decreasing monotonically, ε_i are the range residuals.

In the M-K test, we test the null hypothesis H_0 which says that there is no trend, and the alternative hypothesis H_1 which means that there is a trend in the series. If the results gotten from the test agrees with the null hypothesis (meaning that there is no trend), it means that the given data x_i is randomly ordered in time (t), while the alternative hypothesis says that there is either an increasing monotonic or a decreasing monotonic trend.

The M-K test uses the statistic S, calculated using.

$$S = \sum_{k=1}^{n-1} \sum_{j=k+1}^n \text{sgn}(x_j - x_k) \tag{7}$$

where.

$$\text{sgn}(x_j - x_k) = \begin{cases} +1; & \text{if } (x_j - x_k) > 0 \\ 0; & \text{if } (x_j - x_k) = 0 \\ -1; & \text{if } (x_j - x_k) < 0 \end{cases} \tag{8}$$

The number of data values is represented by n. A positive S value indicates an upward variation, and a negative S value characterizes a downward variation.

The normal approximation (Z statistic) is always used if the number of data values n is from 10 and above. We should also note that when there are tied/equal values, the accuracy of using the Z statistic will reduce if the data values are close to 10.

To compute the value of the Z statistic, the variance of S 'VAR(S)' is used

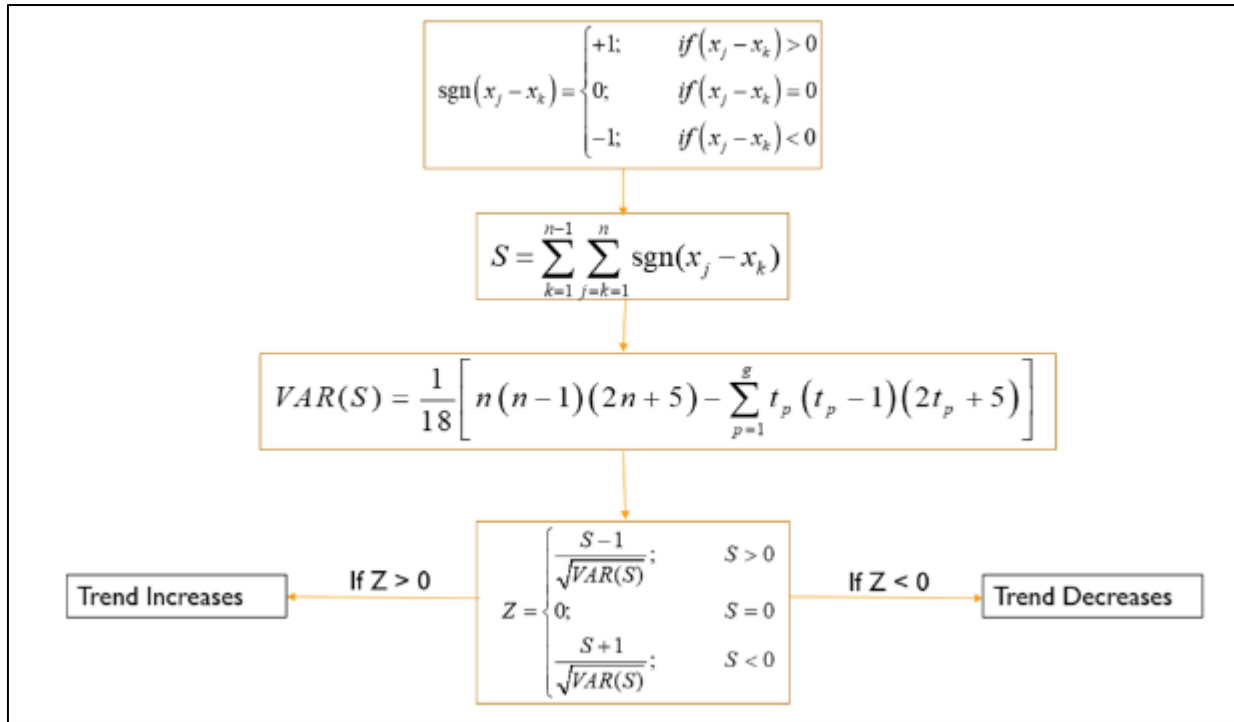
$$\text{VAR}(S) = \frac{1}{18} \left[n(n-1)(2n+5) - \sum_{p=1}^g t_p(t_p-1)(2t_p+5) \right] \tag{9}$$

g represents the number of tied groups in the series (showing that the test takes the tied or equal values into consideration. The number of data values in the pth group is represented by t_p.

The test statistic Z is now obtained using the values of VAR(S) and S;

$$Z = \begin{cases} \frac{S-1}{\sqrt{\text{VAR}(S)}}; & S > 0 \\ 0; & S = 0 \\ \frac{S+1}{\sqrt{\text{VAR}(S)}}; & S < 0 \end{cases} \tag{10}$$

The decreasing variation is discerned from a negative Kendall Z value, and an increasing trend is seen from a positive Z value. Both interpretations can be concluded to have a significant trend if the data's p-value is lower than the significance level (< 5% = 0.05 in this case). The trend is not significant if the p-value is higher than the level of significance.



2.3.2. Sen's Slope Estimator

To estimate the slope of a linear existing trend, the nonparametric Sen method is used. We represent the linear equation by [18]

$$f(t) = Qt + B \tag{11}$$

Here, $f(t)$ is described in equation (10) as a function of time which is continuous increasing or decreasing monotonically and Q is the slope and B is a constant. We get the slope estimate in equation (10) by calculating all the slopes of all data value pairs [19]

$$Q_i = \frac{x_j - x_k}{j - k} \tag{12}$$

Here, $j > k$.

If we have n values x_j in the time series, we get as many as $N = n(n-1)/2$ slope estimates Q_i . The Sen's estimator of slope is the median of these N values of Q_i . The N values of Q_i are ranked from the smallest to the largest and the Sen's estimator is [18-21]

$$Q = \begin{cases} Q_{[(N+1)/2]} & \text{if } N \text{ is odd} \\ \frac{1}{2}Q_{[N/2]} + Q_{[(N+2)/2]} & \text{if } N \text{ is even} \end{cases} \tag{13}$$

A $100(1 - \alpha) \%$ two-sided confidence interval about the slope estimate is obtained by the nonparametric technique based on the normal distribution. The method is valid for n as small as 10 unless there are many groups.

Box Plots

Box plots show a graphical summarization of data; it does not give a detailed representation of the data distribution but gives an indication of the skewness of data. Box plots summarize data in the following way [22].

Lower extreme/minimum ($Q1 - 1.5 \cdot IQR$), Lower quartile ($Q1$), median ($Q2$), upper quartile ($Q3$) and upper extreme ($Q3 + 1.5 \cdot IQR$).

3. Results and Discussion

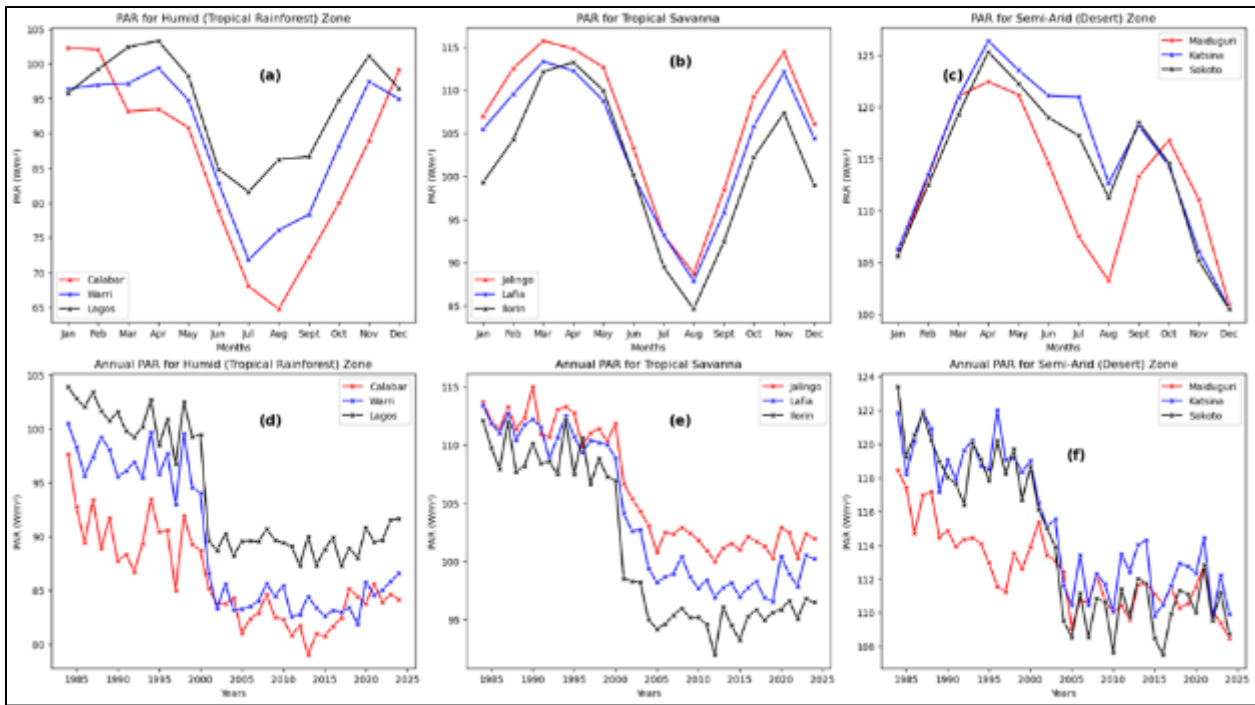


Figure 2(a) to (f) Monthly and Annual trend of PAR across the climatic zones

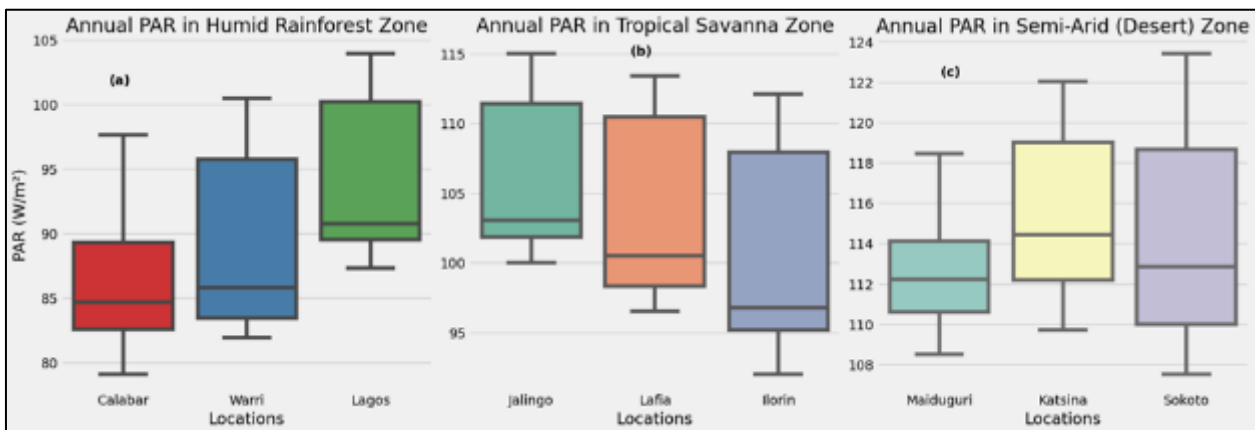


Figure 3a, 3b and 3c illustrate box plots across the climatic zones

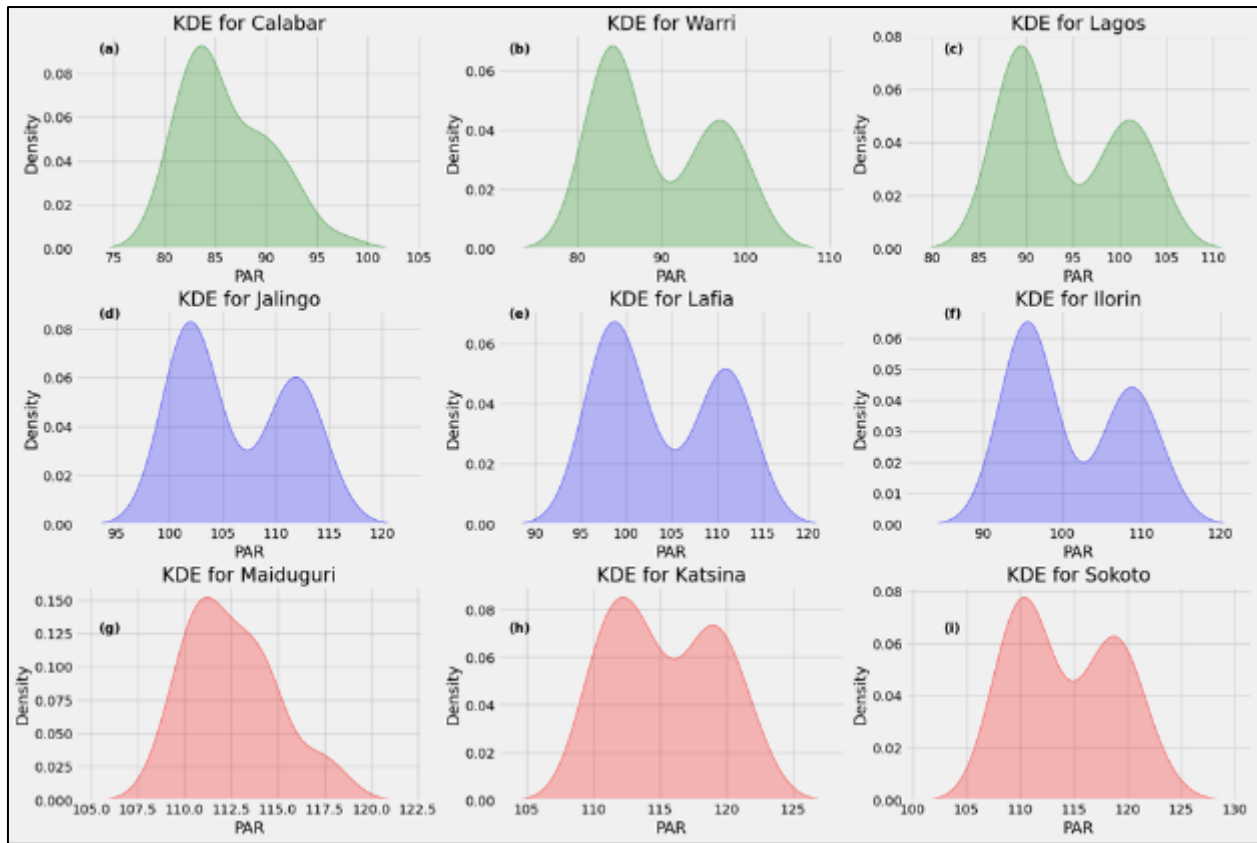


Figure 4 (a) to (i) KDE plot of all the locations across the climatic zones

Table 2 Mann-Kendall and Sen’s estimator trend test for PAR across the climatic zones in Nigeria for 41 years period from 1984 to 2024

Location	Mann Kendall's Statistic (S)	Test Statistic (Z)	p-value (Two-tailed)	Sen's slope (Q)	Test Interpretation	Trend
Calabar	-418	-4.68	2.8e-6	-0.26	True	Decreasing
Warri	-440.0	-4.93	8.1e-7	-0.42	True	Decreasing
Lagos	-450	-5.04	4.5e-7	-0.40	True	Decreasing
Jalingo	-538.0	-6.03	1.6e-9	-0.37	True	Decreasing
Lafia	-559.0	-6.26	3.6e-10	-0.44	True	Decreasing
Ilorin	-446.0	-4.99	5.7e-7	-0.44	True	Decreasing
Maiduguri	-537.0	-6.02	1.7e-9	-0.16	True	Decreasing
Katsina	-489.0	-5.48	4.2e-8	-0.27	True	Decreasing
Sokoto	-506.0	-5.67	1.4e-8	-0.32	True	Decreasing

3.1. Monthly and Annual Distribution of PAR In Nigeria Across the Climatic Zones

Figures 2a–2c highlights the spatial and seasonal variability of Photosynthetically Active Radiation (PAR) across the three major climatic zones of West Africa: Humid, Tropical Savanna and Semi-Arid zone. These variations are largely driven by cloud cover, atmospheric aerosols, water vapor content, solar zenith angle, and latitude.

In the Humid Zone (Figure 2a), comprising Cross River-Calabar, Delta-Warri, and Lagos, PAR values are generally the lowest across all zones, with maximum peaks of 104 W/m^2 in April and November for Lagos, and the lowest values of 81 W/m^2 during the wet season (July), Cross River-Calabar has the lowest PAR of $65\text{--}68 \text{ W/m}^2$ in July and August, while Lagos has its lowest PAR of 72 W/m^2 in July and their maximum values in April and November. The bimodal peak corresponds with the ITCZ's northward and southward passage, typical of the double rainfall maxima in this region. This substantial dip is attributed to dense cloud cover and high rainfall typical of equatorial rainforest climates, which significantly attenuate incoming solar radiation. (Kumar et al., 2019)[23] The Tropical Savanna Zone (Figure 2b) displays slightly higher PAR compared to the Humid zone in 2(a) with dual peaks $116, 114$ and 113 W/m^2 for Jalingo, Lafia and Ilorin in April and October and dip of $85, 87$ and 88 W/m^2 for Ilorin, Lafia and Jalingo in August consistent with the solar equinox periods, and dips in August and December, linked to mid-year rainfall and dry season haze, respectively. The Semi-Arid zone (Figure 2c) displays the highest radiation compared to all the zones with Katsina being the highest with 126 W/m^2 , Sokoto 125 W/m^2 and Maiduguri 123 W/m^2 in April while the lowest was observed in December, August and January. The region has less influence of the Inter Tropical Convergence zone (ITCZ) as the wind from Sahara Desert is predominant.

The annual trends of Photosynthetically Active Radiation (PAR) across West African climatic zones, as shown in Figures 2d–2f, reveal significant spatial and temporal variability driven by atmospheric transparency, cloud cover, latitude, and climatic conditions. The Humid Forest Zone (Figure 2d), including Calabar, Warri, and Lagos, shows the lowest long-term PAR values due to persistent cloud cover and high rainfall. Lagos had the highest PAR in this zone, peaking at 104 W/m^2 in 1984 and declining to 87 W/m^2 by 2015. Warri followed a similar pattern, while Nigeria-Calabar consistently recorded the lowest, declining from 97 W/m^2 in 1984 to 84 W/m^2 in 2024. This supports existing literature that links reduced solar radiation in equatorial zones to higher cloudiness and atmospheric water vapor (Wild et al., 2021; Papachristopoulou et al., 2024) [24][25].

In the Tropical Savanna Zone (Figure 2e), comprising Jalingo, Lafia, and Ilorin, higher PAR values were observed in Jalingo reached 115 W/m^2 in 1990, while all three locations showed a decreasing trend post-2000, likely due to increased aerosol loading and land use changes, aligning with findings by Pinker et al. (2005)[26] on regional solar dimming.

Semi-Arid regions (Figure 2f) such as Katsina, Sokoto, and Maiduguri displayed uniform trends with high PAR values up to 124 W/m^2 in 1984 in Sokoto, suggesting minimal cloud cover and stronger solar irradiance due to dry conditions.

3.2. Box Plots Distribution of PAR Across the Climatic Zones in Nigeria

Figures 3a to 3c illustrate the box plots of Photosynthetically Active Radiation (PAR) across four climatic zones in Nigeria; Humid Zone, Tropical Savanna and Semi-Arid Zone, with data from 9 representative locations. These plots reveal a clear latitudinal and climatic gradient in PAR, increasing from the southern humid regions to the northern arid areas.

In the Humid Zone (Figure 3a), represented by Calabar, Warri, and Lagos, the PAR values are comparatively low, with Calabar showing a median of 85 W/m^2 , Warri at 86 W/m^2 , and Lagos at 92 W/m^2 . The lower whiskers in this zone start as low as 78 W/m^2 in Calabar and 82 W/m^2 in Warri and 87 W/m^2 in Lagos. These values are influenced by dense cloud cover and high rainfall, which limit solar penetration. While such conditions favor shade-tolerant and moisture-loving crops like cocoa, yam, and plantain, the relatively low PAR can hinder light-dependent crops like maize and rice, particularly during extended wet seasons, leading to delayed flowering and reduced yields.

Moving to the Tropical Savanna Zone (Figure 3b), which includes Jalingo, Lafia, and Ilorin, there is a noticeable increase in PAR. Jalingo shows a median PAR of 103 W/m^2 , Lafia 100 W/m^2 , and Ilorin 97 W/m^2 . This zone experiences a balance between sunlight and rainfall, supporting a wide variety of crops, including maize, millet, cassava, sorghum, and legumes. The combination of adequate PAR (ranging from 97 to 115 W/m^2) and seasonal rainfall offers favorable photosynthetic conditions, especially during the growing season. Consequently, this zone is among the most agriculturally productive in the region.

The Semi-Arid Zone (Figure 3c), comprising Katsina, Sokoto, and Maiduguri, exhibits even higher PAR levels. Median values here reach 114.5 W/m^2 in both Katsina and Sokoto 113.5 W/m^2 , and 112 W/m^2 in Maiduguri. The whiskers in Sokoto extend as high as 123 W/m^2 . These values fall within or slightly above the optimum PAR range for photosynthesis, generally cited as $100\text{--}120 \text{ W/m}^2$ for most crops (Monteith, 1977; Mekouar, 2024)[7][27]. While high PAR supports rapid crop growth, the short rainy season and high evapotranspiration rates pose serious risks. Crops like sorghum, millet, and cowpea thrive when rainfall coincides with high PAR, but in dry years, the lack of moisture can

lead to leaf scorch, reduced chlorophyll efficiency, and lower grain fill, undermining yields despite abundant solar energy.

3.3. Kernel density estimation for PAR

Figures 4a–4i present Kernel Density Estimation (KDE) plots of Photosynthetically Active Radiation (PAR) across Nigeria's three major climatic zones, showing clear spatial gradients that directly influence agricultural productivity.

In the humid tropical rainforest zone (Figures 4a–4c), Calabar showed a unimodal peak at $\sim 84 \text{ W/m}^2$, Warri had a bimodal pattern (85 W/m^2 and 95 W/m^2), and Lagos also bimodal ($\sim 89 \text{ W/m}^2$ and 101 W/m^2). The lower PAR levels in Calabar reflect persistent cloud cover and high atmospheric moisture, reducing light availability via scattering and absorption. While such conditions support shade-tolerant crops like cocoa, coffee, and leafy vegetables, they may limit yields of high-light-demand crops (e.g., maize) unless cultivated in drier months or with canopy management.

In the tropical savanna zone (Figures 4d–4f), Jalingo peaked at 102 W/m^2 and 112 W/m^2 , Lafia at 100 W/m^2 and 112 W/m^2 , and Ilorin at 95 W/m^2 and 109 W/m^2 . The higher dry-season PAR values favor crops such as sorghum, maize, and groundnuts, which thrive under strong sunlight, though supplemental irrigation may be required to counter dry-season water deficits.

In the semi-arid zone (Figures 4g–4i), Maiduguri had a unimodal peaked at 111 W/m^2 , Katsina at 112 W/m^2 and 119 W/m^2 , and Sokoto at 110 W/m^2 and 119 W/m^2 . High PAR here enhances photosynthesis for cereals like millet and sorghum, but the combination of intense radiation and low humidity increases evapotranspiration, risking water stress without drought-adaptive practices.

3.4. Mann-Kendall and Sen's slope Trend Test of PAR Across Nigeria Climatic Zones

The analysis of long-term trends in Photosynthetically Active Radiation (PAR) across Nigeria reveals significant spatial and temporal variability shaped by climatic conditions. As shown in Table 2, the application of the non-parametric Mann-Kendall trend test and Sen's slope estimator across different climatic zones Humid, Tropical Savanna, Semi-Arid, and Arid provides insights into the direction and magnitude of change in PAR over time.

Focusing on the Humid Zone, which includes Calabar, Warri, and Lagos, all three locations exhibit a statistically significant decreasing trend in PAR. In Calabar, a p-value of 2.8×10^{-6} and a z-value of -4.68 suggest a highly significant negative trend, with a Sen's slope of -0.26 W/m^2 per year. This indicates a consistent annual decline in PAR likely driven by increased cloudiness or atmospheric moisture typical of the coastal rainforest zone.

Similarly, Warri demonstrates a more pronounced trend, with a p-value of 8.1×10^{-7} , z-value of -4.93 , and Sen's slope of -0.42 W/m^2 per year, showing a faster reduction in incoming PAR. Lagos, with a p-value of 4.5×10^{-7} , z-value of -5.04 , and Sen's slope of -0.40 W/m^2 per year, records the steepest rate of decline in the Humid Zone.

In the Tropical Savanna Zone, which includes Jalingo, Lafia, and Ilorin, all three locations show statistically significant negative trends in PAR, indicating a steady decline in photosynthetically active radiation. Lafia presents the strongest signal, with a z-value of -6.26 , p-value of 3.6×10^{-10} , and Sen's slope of $-0.44 \text{ W/m}^2/\text{year}$, suggesting a notable drop in radiation input over the years. Similarly, Jalingo records a z-value of -6.03 , p-value of 1.6×10^{-9} , and slope of $-0.37 \text{ W/m}^2/\text{year}$, while Ilorin shows a z-value of -4.99 , p-value of 5.7×10^{-7} , and slope of $-0.44 \text{ W/m}^2/\text{year}$. These declines could adversely affect staple crops such as maize, millet, and groundnut, especially during key growth stages where sufficient light is essential for photosynthesis and biomass accumulation.

The Semi-Arid Zone, comprising Maiduguri, Katsina, and Sokoto, also exhibits significant downward trends in PAR. Katsina shows a z-value of -5.48 , p-value of 4.2×10^{-8} , and slope of $-0.27 \text{ W/m}^2/\text{year}$. Maiduguri follows with a z-value of -6.02 , p-value of 1.7×10^{-9} , and slope of $-0.16 \text{ W/m}^2/\text{year}$, while Sokoto has a z-value of -5.67 , p-value of 1.4×10^{-8} , and slope of $-0.32 \text{ W/m}^2/\text{year}$. These reductions in PAR could hinder crop performance in already moisture-limited environments. Crops like sorghum and cowpea, which are adapted to high radiation and water stress, may experience yield reduction, especially under conditions of compounded drought and reduced solar input.

4. Conclusion

This study assessed long-term trends in Photosynthetically Active Radiation (PAR) across Nigeria's three main climatic zones Humid Tropical Rainforest, Tropical Savanna, and Semi-Arid Sahel using 41 years (1984–2024) of satellite data and robust statistical analysis. Trends show a consistent and statistically significant declining trend of PAR across all

regions, with rates ranging from 0.16 to 0.44 W/m² per year. It has decreased because of increasing cloud cover, aerosols, dust events, and land use changes. Temporally, the Humid Zone exhibited the minimum PAR due to the persistent rainfall and cloudiness, while the Tropical Savanna recorded intermediate levels of PAR that offer radiation and rain balancing to enable crops varieties. The Semi-Arid Zone experienced the maximum PAR but faces the risk of declining rainy seasons and high evapotranspiration, which increases its vulnerability to water stress and crop damage. Overall, the reduction in PAR jeopardizes agricultural production, food safety, and ecosystem stability in Nigeria, and adaptive agriculture practices and policy measures become a necessity.

Compliance with ethical standards

Acknowledgement

The authors express sincere gratitude to the National Aeronautics and Space Administration (NASA) for providing the satellite-based PAR datasets used in this research. Appreciation is also extended to the University of Calabar and the University of Cross River State, Calabar, for their institutional support and research facilities. Special thanks to colleagues and collaborators whose insights and contributions enhanced the quality of this work.

Disclosure of conflict of interest

No conflict of interest to be disclosed.

References

- [1] Lobell, D. B., & Field, C. B. (2007). Global scale climate–crop yield relationships and the impacts of recent warming. *Environmental Research Letters*, 2(1), 014002. <https://doi.org/10.1088/1748-9326/2/1/014002>
- [2] Adejuwon, J. (2006). Food crop production in Nigeria. II. Potential effects of climate change. *Climate Research*, 32, 229–245. <https://doi.org/10.3354/cr032229>
- [3] Weatherhead, E. C., Wielicki, B. A., Ramaswamy, V., Abbott, M., Ackerman, T. P., Atlas, R., Brasseur, G., Bruhwiler, L., Busalacchi, A. J., Butler, J. H., Clack, C. T. M., Cooke, R., Cucurull, L., Davis, S. M., English, J. M., Fahey, D. W., Fine, S. S., Lazo, J. K., Liang, S., ... Wuebbles, D. (2018). Designing the Climate Observing System of the Future. *Earth's Future*, 6(1), 80–102. <https://doi.org/10.1002/2017EF000627>
- [4] Sultan, B., Defrance, D., & Iizumi, T. (2019). Evidence of crop production losses in West Africa due to historical global warming in two crop models. *Scientific Reports*, 9(1), 12834. <https://doi.org/10.1038/s41598-019-49167-0>
- [5] Nicholson, S. E. (2013). The West African Sahel: A Review of Recent Studies on the Rainfall Regime and Its Interannual Variability. *ISRN Meteorology*, 2013, 1–32. <https://doi.org/10.1155/2013/453521>
- [6] Roderick, M. L., Farquhar, G. D., Berry, S. L., & Noble, I. R. (2001). On the direct effect of clouds and atmospheric particles on the productivity and structure of vegetation. *Oecologia*, 129(1), 21–30. <https://doi.org/10.1007/s004420100760>
- [7] Monteith, J. L. (1972). Solar Radiation and Productivity in Tropical Ecosystems. *The Journal of Applied Ecology*, 9(3), 747. <https://doi.org/10.2307/2401901>
- [8] Zhao, M., & Running, S. W. (2010). Drought-Induced Reduction in Global Terrestrial Net Primary Production from 2000 Through 2009. *Science*, 329(5994), 940–943. <https://doi.org/10.1126/science.1192666>
- [9] Thomas, C., Wandji Nyamsi, W., Arola, A., Pfeifroth, U., Trentmann, J., Dorling, S., Laguarda, A., Fischer, M., & Aculinin, A. (2023). Smart Approaches for Evaluating Photosynthetically Active Radiation at Various Stations Based on MSG Prime Satellite Imagery. *Atmosphere*, 14(8), 1259. <https://doi.org/10.3390/atmos14081259>
- [10] Junior, P. A., Quansah, E., & Dogbey, F. (2022). Satellite-based estimates of photosynthetically active radiation for tropical ecosystems in Ghana—West Africa. *Tropical Ecology*, 63(4), 615–625. <https://doi.org/10.1007/s42965-022-00234-0>
- [11] Drame, M., Ceamanos, X., Roujean, J., Boone, A., Lafore, J., Carrer, D., & Geoffroy, O. (2015). On the Importance of Aerosol Composition for Estimating Incoming Solar Radiation: Focus on the Western African Stations of Dakar and Niamey during the Dry Season. *Atmosphere*, 6(11), 1608–1632. <https://doi.org/10.3390/atmos6111608>

- [12] Ayanlade, A., Atai, G., & Jegede, M. O. (2019). Spatial and seasonal variations in atmospheric aerosols over Nigeria: Assessment of influence of intertropical discontinuity movement. *Journal of Ocean and Climate: Science, Technology and Impacts*, 9, 1759313118820306. <https://doi.org/10.1177/1759313118820306>
- [13] Clauzel, L., Anquetin, S., Lavaysse, C., Bergametti, G., Bouet, C., Siour, G., Lapere, R., Marticorena, B., & Thomas, J. (2025). Solar radiation estimation in West Africa: Impact of dust conditions during the 2021 dry season. *Atmospheric Chemistry and Physics*, 25(2), 997–1021. <https://doi.org/10.5194/acp-25-997-2025>
- [14] Antón, M., Sorribas, M., Bennouna, Y., Vilaplana, J. M., Cachorro, V. E., Gröbner, J., & Alados-Arboledas, L. (2012). Effects of an extreme desert dust event on the spectral ultraviolet irradiance at El Arenosillo (Spain). *Journal of Geophysical Research: Atmospheres*, 117(D3), 2011JD016645. <https://doi.org/10.1029/2011JD016645>
- [15] Udo, S. O., & Aro, T. O. (1999). Global PAR related to global solar radiation for central Nigeria. *Agricultural and Forest Meteorology*, 97(1), 21–31. [https://doi.org/10.1016/S0168-1923\(99\)00055-6](https://doi.org/10.1016/S0168-1923(99)00055-6)
- [16] Mann, H. B. (1945). Nonparametric Tests Against Trend. *Econometrica*, 13(3), 245. <https://doi.org/10.2307/1907187>
- [17] Phuong, D. N. D., Tram, V. N. Q., Nhat, T. T., Ly, T. D., & Loi, N. K. (2020). Hydro-meteorological trend analysis using the Mann-Kendall and innovative- τ methodologies: A case study. *International Journal of Global Warming*, 20(2), 145. <https://doi.org/10.1504/IJGW.2020.105385>
- [18] Sen, P. K. (1968). Estimates of the regression coefficient based on Kendall's tau. *Journal of the American statistical association*, 63(324), 1379-1389.
- [19] [19]Agbo, E. P., Ekpo, C. M., & Edet, C. O. (2020). *Trend Analysis of Meteorological Parameters, Tropospheric Refractivity, Equivalent Potential Temperature for a Pseudoadiabatic Process and Field Strength Variability, Using Mann Kendall Trend Test and Sens Estimate* (Version 1). arXiv. <https://doi.org/10.48550/ARXIV.2010.04575>
- [20] Kisi, O., & Ay, M. (2014). Comparison of Mann–Kendall and innovative trend method for water quality parameters of the Kizilirmak River, Turkey. *Journal of Hydrology*, 513, 362–375. <https://doi.org/10.1016/j.jhydrol.2014.03.005>
- [21] UU, A., Yusuf, A. S., Edet, C. O., Oche, C. O., & Agbo, E. P. (2018). Trend analysis of temperature in Gombe state using Mann Kendall trend test.
- [22] Okono, M. A., Agbo, E. P., Ekah, B. J., Ekah, U. J., Ettah, E. B., & Edet, C. O. (2022). Statistical Analysis and Distribution of Global Solar Radiation and Temperature Over Southern Nigeria. *Journal of the Nigerian Society of Physical Sciences*, 588. <https://doi.org/10.46481/jnsps.2022.588>
- [23] Kumar, S., Srivastava, A. K., Pathak, V., Bisht, D. S., & Tiwari, S. (2019). Surface solar radiation and its association with aerosol characteristics at an urban station in the Indo-Gangetic Basin: Implication to radiative effect. *Journal of Atmospheric and Solar-Terrestrial Physics*, 193, 105061. <https://doi.org/10.1016/j.jastp.2019.105061>
- [24] Wild, M., Wacker, S., Yang, S., & Sanchez-Lorenzo, A. (2021). Evidence for Clear-Sky Dimming and Brightening in Central Europe. *Geophysical Research Letters*, 48(6), e2020GL092216. <https://doi.org/10.1029/2020GL092216>
- [25] Papachristopoulou, K., Fountoulakis, I., Bais, A. F., Psiloglou, B. E., Papadimitriou, N., Raptis, I.-P., Kazantzidis, A., Kontoes, C., Hatzaki, M., & Kazadzis, S. (2024). Effects of clouds and aerosols on downwelling surface solar irradiance nowcasting and short-term forecasting. *Atmospheric Measurement Techniques*, 17(7), 1851–1877. <https://doi.org/10.5194/amt-17-1851-2024>
- [26] Pinker, R. T., Zhang, B., & Dutton, E. G. (2005). Do satellites detect trends in surface solar radiation?. *Science*, 308(5723), 850-854.
- [27] Mekouar, M. A. (2024). Food and Agriculture Organization of the United Nations (FAO). *Yearbook of International Environmental Law*, 34(1), yvae031. <https://doi.org/10.1093/yiel/yvae031>